A Fracture Mechanics Approach to the Repair of Ferritic Stainless Steel Castings by Welding

Stress relief treatment should follow welding repairs to help improve the fracture toughness of the weld metal

BY K. PURAZRANG

Introduction

Defects such as shrinkage porosity, hot tears, slag, cracks, etc. may be introduced during casting. These discontinuities can act as stress raisers, thereby reducing fatigue life and ductility of the casting. Therefore, defect tolerance levels for fracture safe design have been specified and unacceptable defects detected removed and repaired with high integrity weld metal. However, in most cases little attention has been paid to checking the toughness and allowable defect dimension of the repair weld. In cases where the weld metal or heat-affected zone (HAZ) contains cracks of critical order which cannot be detected by means of the available NDT test methods, repair of the casting will not have reduced the danger of fracture in service and no improvement will have been achieved. Consequently, a successful upgrading of the casting can only be made when detailed information on the metallurgical and mechanical properties of the casting, HAZ, and repaired weld metal, has been provided.

This paper is concerned with investigation into the relative toughness parameters of 13% Cr, 6% Ni and 0.5% Mo steel castings and a typical weld metal used for aluminum-killed steel. The artificial defect was simulated by the means of a gouging procedure, and weld repairs were carried out according to the production welding plan.

K. PURAZRANG is Head of the Metallurgical Engineering Department, Arya-Mehr University of Technology, Tehran, Iran.

Experimental Methods

Materials and Welding Procedure

The casting material studied in this investigation was a hardenable stainless steel which has been used for water turbines and similar castings. The steel has been reported[1,2] to have excellent impact properties in addition to good weldability in cold condition. The filler metal (i.e., electrode) used to repair this material was Metrode 13.4 Mo.L.R. The chemical compositions of casting and filler metal are shown in Table 1.

Two cast test blocks—each 400 × 130 × 140 mm (approximately 15¾ × 5½ × 5½ in.)—were produced from commercial melts and were heat treated with a production casting at all stages during fettling. The final heat treatment was normalized at 950 C (1742 F) for 16 hours (h) and double tempered at 600 C (1112 F) for 16 h furnace cooling to 250 C (482 F) and at 600 C (1112 F) for 16 h furnace cooling to room temperature respectively. A groove approximately 55 mm deep was excavated by the means of an air carbon-arc gouging technique along one side of both blocks. The grooves were hand ground before each was filled with the electrode, using a stringer bead technique. The electrodes were baked at approximately 200 C (392 F) for 1 h prior to use, and the heat input used during the welding process was within the range 21.6–25.2 kJ per centimeter. The preheat and interpass temperature was kept at 180–210 C (356–410 F) using a contact thermocouple.

Table 1—Chemical Compositions, wt-%

	C	Mn	Si	S	P	Cr	Ni	Mo	Cu	Al
Casting	0.04	0.65	0.60	0.025	0.012	13.2	5.76	0.49	0.06	0.052
Metrode Mo. L.R. weld metal	0.057	0.66	0.36	0.010	0.019	12.40	3.95	0.50	0.05	–

Table 2—Tensile Properties of Material Tested

Material	$\sigma_{0.2}$, N/mm²	Ultimate tensile strength, N/mm²	Elongation (lo = 5do), %
Casting[a]	650	781.2	10
HAZ[a]	946.2	977.9	4.5
Weld Met[a]	956.25	1038.7	2.5
Casting[b]	650	809.7	12
HAZ[b]	701.7	795.5	4.5
Weld Met[b]	735	880	12

[a] After welding and before stress relief heat treatment.
[b] After stress relief heat treatment.

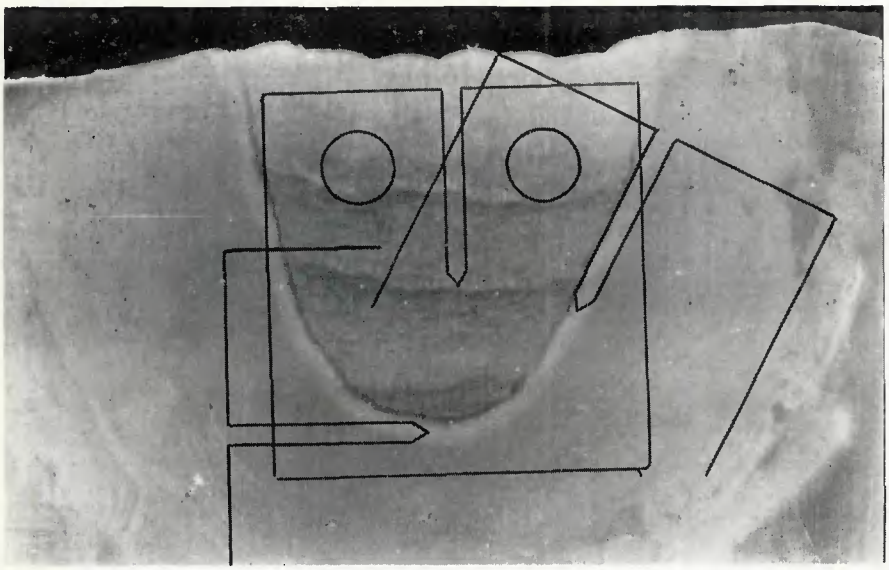

Fig. 1—Locations of extracted specimens from the weld metal and from the HAZ area

One block was investigated as welded while the other one was first stress relieved for 12 h at 600 C (1112 F) following furnance cooling. Hounsfield tensile specimens were machined from the weld, casting and the HAZ before and after stress relief heat treatment. In order to make sure that extracted specimens from the HAZ were located in the proper area, modified Hounsfield tensile specimens of 3½ mm (0.14 in.) gauge diameter have been used. The results of tensile tests have been collected in Table 2.

Fracture Toughness Tests

The 25 mm (1 in.) thick compact tension fracture toughness specimens were machined from the weld, casting and HAZ. The locations of specimens are illustrated in Fig. 1. The specimens were machined so that subsequent fatigue pre-cracks were located right in the weld metal, casting or HAZ area. In order to simulate the possible HAZ cracks, two types of specimen were machined from the appropriate area of HAZ around the weld metal which may generally represent HAZ cracks of the toe and underbead types.

All tests were carried out at room temperature using a 50t Denison testing machine. A slow crosshead speed of approximately 0.5 mm/min (0.02 in./min) during elastic loading was used. Autographic records were obtained of applied load against the output from a linear displacement clip gauge mounted on knife edges at the open end of the machine notch.

The assessment of fracture properties of materials tested was based on linear elastic fracture mechanics and general yielding fracture mechanics analyses, depending upon the results obtained. The BS/ASTM criterion expression 2.5 $(K_Q/\alpha_y)^2$ was calculated and compared with crack length and specimen thickness.[3] Where linear elastic analyses were invalidated by the onset of yielding, the amount of pre-fracture ductility, measured as a critical crack opening displacement (COD) was used as an alternative fracture toughness parameter.[4] The minimum allowable defect sizes were derived from the results obtained to estimate the likelihood of fracture in the material and condition tested.

Fractography and Fracture Mechanism

The fracture surfaces of broken specimens were carefully examined using a scanning electron microscope. The detail of various specimens before and after stress relief treatment are compared in Figs. 2–5.

There was not much difference between fracture appearance of the casting before and after stress relieving. The simple microvoidal coalescence mode of fracture which nucleated around inclusions predominated throughout the casting—Fig. 2. The analysis of inclusions by the means of the electron probe microanalyzer attached to the scanning electron microscope indicated that they were mainly manganese sulphide. Some regions of fine microporosity were also observed.

The fracture mechanism of the weld metal has been widely affected by the stress relieving treatment. While the fracture mechanism of the weld metal before stress relieving has been principally by cleavage fracture with some microvoidal coalescence, the fracture surface after stress relieving consisted of fine microvoidal coalescence which

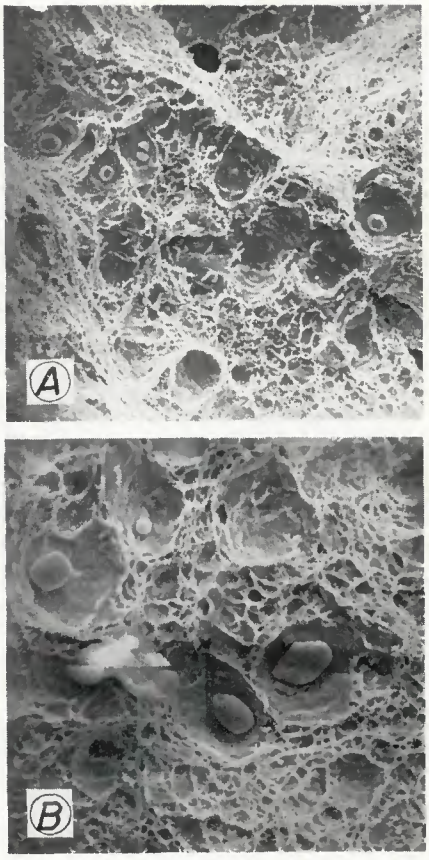

Fig. 2—Microvoidal coalescence mode of fracture in casting: A—before stress relief treatment, X550; B—after stress relief treatment, ×1100 (A and B reduced 38% on reproduction)

was very similar in appearance over the whole fracture surface—Fig. 3.

The micromechanism of the HAZ fracture before stress relief treatment was small cleavage facets of the martensite platelets which have been separated by ridges. After stress relieving, the fracture surface consisted predominantly of equiaxed dimples and moderately large dimples containing inclusions but some local cleavage facets were also discernible—Fig. 4.

Figure 5A shows that the fracture surface in the HAZ in the underbead area appears to have propagated by a mixture of intergranular separation, cleavage fracture and macrovoidal coalescence. Macrovoids have been initiated at interfaces between the matrix and inclusions and may have been also initiated at regions of fine microporosity. The low energy fracture may have been due to the increasing local yield stress and increasing magnitude of cleavage stress resulting from work-hardening and constraint effect.

The fracture surface of a stress relieved specimen from the same area showed mixed mechanisms of dimpled rupture, intergranular rupture and quasi-cleavage—Fig. 5B. This mixed mode fracture may be referred to the microstructural history of HAZ which

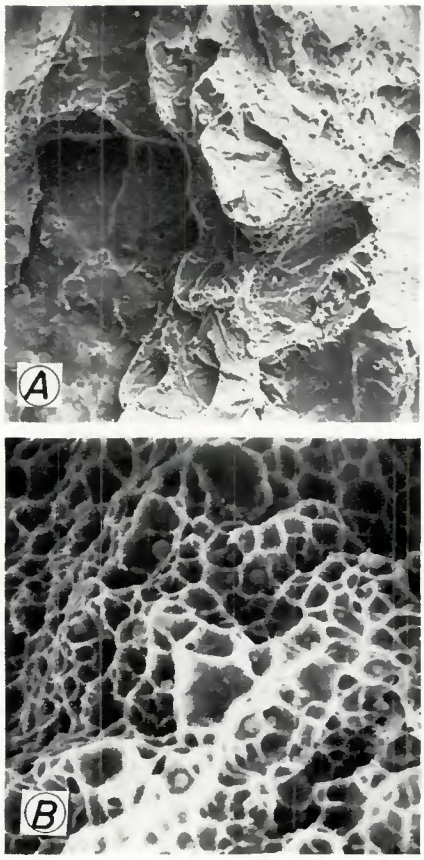

Fig. 3—Fracture surface of weld metal: A—before stress relief treatment, ×550; B—after stress relief treatment, ×2500 (A and B reduced 38% on reproduction)

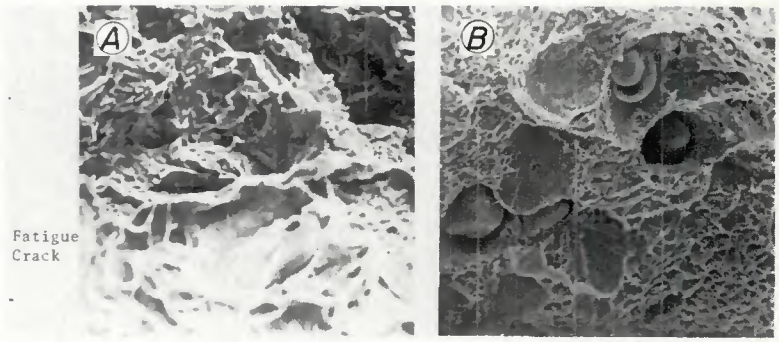

Fig. 4—Fractographs of HAZ area of toe crack: A—before stress relief treatment, ×1150; B—after stress relief treatment, ×1100 (A and B reduced 50% on reproduction)

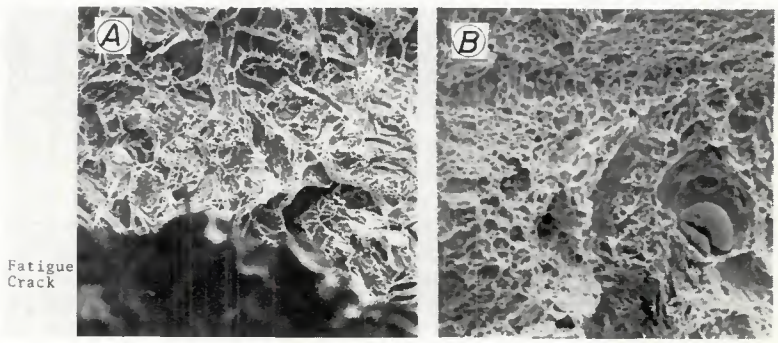

Fig. 5—Fracture surface of HAZ area of underbead area: A—before stress relief treatment, ×525; B—after stress relief treatment, ×1100 (A and B reduced 50% on reproduction)

was tempered martensite with large grain size with fine microporosity. Again, microvoids have been initiated at the interfaces between the matrix and inclusions and also in regions of fine microporosity. Intergranular rupture may have been produced by the separation of grain boundaries and possibly by coalescence of microvoids. Quasi-cleavage fractures are believed to be related to the tempered martensite structure of HAZ area.

Metallography

The microstructure of the casting, HAZ and weld metal were examined before and after stress relieving. The microstructure of the casting consisted of coarse upper bainite in a tempered matrix and that from HAZ area of coarse martensite laths. After welding the microporosities were finely distributed, but occasionally larger porosities were also observed—Fig. 6. The microstructure of the weld metal at this stage is shown in Fig. 6D; it appears to be coarse bainite.

After 12 h at 600 C (1112 F) the coarse upper bainite microstructure of the casting was tempered thoroughly while that from the weld metal still contained some coarse bainite—Figs. 7A and B. The microstructure of the heat-affected zones at this stage consisted of tempered martensite as shown in Fig. 7C.

Discussion

The main advantage of the fracture mechanics approach to materials assessment is the possibility of calculating the flaw size necessary to cause failure when fracture toughness data such as K_{Ic}, δ_c or δ_{max} together with the stress applied to the component and the nature of the stress are known.

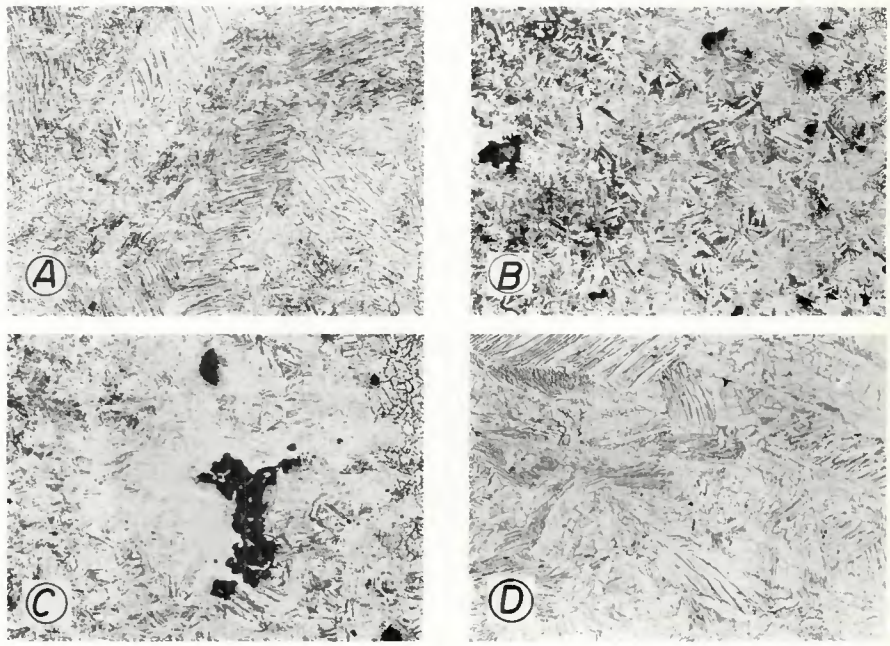

Fig. 6—Microstructures of 13% Cr-6% Ni material before stress relieving: A—with upper bainite in a lightly tempered condition; B—martensitic microstructure of HAZ area; C—large inclusion in microstructure of HAZ; D—typical microstructure of Metrode 13.4 Mo.L.R. weld metal showing coarse bainite. ×140 (reduced 38% on reproduction)

Fig. 7—Microstructures after 12 hours at 600 C (1112 F): A—fully tempered microstructure close to crack tip, ×320; B—weld in stress relieved condition still containing some upper bainite, ×320; C—HAZ after stress relieving and consisting of tempered martensite, ×280. (A, B and C reduced 33% on reproduction)

Table 3—Allowable Defect Sizes of Investigated Materials[a]

Material	$\sigma_{0.2}$, n/mm²	$\sigma_D/0.2$[b]	K_M, MN • m$^{-3/2}$	δ_{max}, mm	Allowable defect in 100 mm thickness, mm	
					Depth	Length
Casting[c]	650	0.66	152.6	0.47	48	230
HAZ[c],[e]	946.9	1.45+	122.3	0.226	12	60
HAZ[c],[f]	946.9	1.45+	166.1	0.29	13.5	67.5
Weld metal[c]	956.2	1.45+	99.5	0.162	5.5	27.5
Casting[d]	650	0.66	145	0.485	49	245
HAZ[d],[e]	701.7	0.617	146.6	0.415	47	235
HAZ[d],[f]	701.7	0.617	147.5	0.416	47	235
Weld metal[d]	735	0.589	135.2	0.285	38	190

[a] S_{max}—fracture toughness criterion used.
[b] Design stress = 433.3 N/mm² + assuming yield point residual stress.
[c] After welding and before stress relief heat treatment.
[d] After stress relief heat treatment.
[e] Fatigue crack represented by toe-type crack in HAZ area.
[f] Fatigue crack represented by underbead type of crack in HAZ area.

Depending upon the type of behavior of the material, K_{Ic} and δ_c can be used for a realistic calculation of permitted defect size for practical applications; δ_{max}, referring to the crack opening displacement at maximum load, may be used for assessment of the allowable defect size for the purposes of material comparison,[4,5] but usually is relevant to the section size actually tested.

The material tested did not satisfy the BS/ASTM criterion for plain strain conditions, and instruments to monitor the initiation of crack extension were lacking. Consequently, δ_{max} measurements were used to calculate an allowable defect size for the casting, weld metal and HAZ both before and after stress relief.

A number of publications have proposed methods of calculating allowable defect sizes from fracture mechanics data,[6-7] the allowable size being approximately twice the critical size. These present calculations have been carried out on the basis of recent publications, in particular two references,[6,7] assuming static loading and an applied stress of two thirds of 0.2σ of the casting throughout the calculation. It is also necessary to point out that for calculation of allowable defect size a semi-elliptical surface defect, with an aspect ratio of 5:1 in a 100 mm (3.9 in.) thick section has been considered.

The results of the calculation presented in Table 3 show that the largest permissible defect size of 48 mm depth in the casting decreases approximately to 12 mm (0.47 in.) in the HAZ area and 5.5 mm (0.22 in.) in the weld metal before stress relief treatment took place. There were no major differences between the permissible defect dimensions in HAZ areas. The small difference may have been due to the more effective tempering by means of heat released during successive weld runs for that underbead area than the area of the toe.

As can be seen from Table 3, these small differences have been completely eliminated when specimens were tested after stress relief treatment. The allowable defect sizes of the weld metal and the HAZ areas were considerably improved through stress relieving, but the permitted defect size in the weld metal is three-quarters of that permitted in the casting. The comparison of results obtained indicates that when defects are removed from the casting to maintain fitness for purpose the fracture toughness of the weld metal has to be considered. This was also concluded for a Q1N casting.[8]

Referring to Table 3, the fracture toughness of the weld metal at maximum load before stress relieving was very close to the plain strain fracture toughness of K_{Ic}, when the

$$2.5 \left(\frac{K_Q}{\sigma_y}\right)^2$$

criterion was considered. The shape of the load-COD plot for the weld metal in this state had a shape characteristic of brittle fracture. In this case the allowable defect size of the weld metal was ⅑ of that of the casting which may lead to serious reduction in fitness for purposes when an acceptable defect in the casting is removed; the repair weld contains a small defect which may be undetectable and yet still large enough to cause failure of the brittle weld.

Conclusion

The problem of defect tolerance in a 13% Cr-6% Ni hardenable stainless steel casting was investigated by the means of fracture mechanics technology. The fracture toughness of the casting, electrode (filler metal), and HAZ of two important locations—namely the underbead and toe areas as-welded and after stress relieving—were obtained. Allowable defect sizes of investigated materials under

conditions tested have also been calculated.

The results indicated that there were major differences in the values of allowable defect size of casting, HAZ area and weld metal in as-welded condition. Stress relief treatment improved the toughness of HAZ area and the weld metal, but allowable defect size in weld metal was still ¾ of that in the casting. Therefore, it is suggested that to successfully weld repair an unacceptable defect in a casting, the fracture toughness of the weld metal rather than that of the casting has to be considered. However, a stress relief treatment should follow the welding repair to help improve the fracture toughness of the weld metal and improve its fitness for the intended purpose.

Acknowledgment

The author would like to thank: Professor M.B. Waldron for his kindly support of this project, Mr. W.H. Eaton for his guidance, staff of the British steel corporation—Sheffield Laboratories—for their interesting discussion, and BSC Craigneuk Works for supplying the materials used in this study.

References

1. Baggstroem, G., "New Steel for Turbine Runners," *Water Power* 16, 1964, 12, pp. 516-521.

2. Arwidson, S., Baggstrom, G., and Hellmer, L., "New Steels for Power Industry," Iron and Steel Institute publication 117, 1969.

3. BS DD3 "Methods for Plane Strain Fracture Toughness Testing," Draft for development, British Standards Institution, London, 1971.

4. BS DD19 "Methods for Crack Opening Displacement (COD) Testing," Draft for development, British Standards Institution, London, 1972.

5. Barr, R. R., *et al.*, "The Measurement of COD and Its Application to Defect Significance," *Metal Constr.*, 7 (12), 1975, pp. 604-12.

6. BS Committee WEE 37, "Rules for the Derivation of Acceptance Levels for Defects in Fusion Welded Joints," Draft for public comment, British Standards Institution, London, 1976.

7. IIS/IIW—471—74, "Proposed Assessment Methods for Flaws with Respect to Failure," *Welding in the World*, Volume 13, No. 1/2, 1975, pp. 29-48.

8. Webster, S.E., Banks, T.M., and Walker, E.G., "Application of Fracture Mechanics to Weld Repair Toughness in Steel Castings," Welding of Casting International Conference, Paper 12.